ACS APPLIED MATERIALS & INTERFACES

Research Article

Cite This: ACS Appl. Mater. Interfaces 2019, 11, 27568−27573

www.acsami.org

Dual Signal Amplification by eATRP and DNA-Templated Silver Nanoparticles for Ultrasensitive Electrochemical Detection of Nucleic Acids

Haobo Sun,[†] Jinming Kong,*[,†] Qiangwei Wang,[†] Qianrui Liu,[†] and Xueji Zhang*[,‡]

[†]School of Environmental and Biological Engineering, Nanjing University of Science and Technology, Nanjing 210094, P. R. China

[‡]School of Biomedical Engineering, Shenzhen University Health Science Center, Shenzhen, Guangdong 518060, P. R. China

Supporting Information

ABSTRACT: Herein, an ultrasensitive and novel platform for DNA detection is reported, which combines DNA-templated silver nanoparticles (AgNPs) with electrochemical atom transfer radical polymerization signal amplification. Peptide nucleic acid (PNA) functionalized with thiol was modified to the Au electrode surface as a probe to specifically capture target DNA (T-DNA). After Zr^{4+} binds to phosphate on DNA, the initiator [α-bromophenylacetic acid (BPAA)] of ATRP is attached to PNA/DNA heteroduplexes based on the phosphate groups of T-DNA and carboxylate groups of BPAA via zirconium−phosphate−carboxylate chemistries. A large number of glycosyloxyethyl methacrylates (GEMA) were captured on the formed PNA/DNA duplex via ATRP. Afterwards, the polysaccharides were oxidized to polymerized aldehydes with sodium periodate ($NaIO_4$). In addition, AgNPs were deposited on the electrode surface by silver mirror reaction. The results indicate that the amount of AgNPs proportional to the T-DNA was quantified through differential pulse voltammetry. Furthermore, it proves that the modified electrode has good performance in DNA detection, indicating that the DNA sensor has high selectivity, high sensitivity, and stable repeatability. Under the optimal conditions, a good linear relationship is obtained in the range of 10 aM to 10 pM with the correlation coefficient of 0.992, and the detection limit is calculated to be as low as 4.725 aM. In addition, the sensor is successfully used to detect DNA in actual serum samples with satisfactory results, which indicates huge promise for detecting gene biomarkers and clinical analysis.

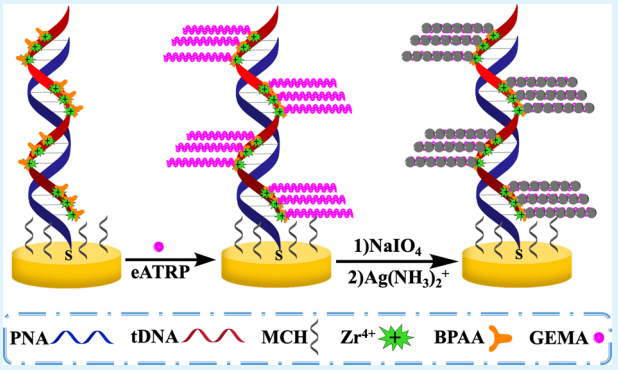

KEYWORDS: *DNA detection, SI-eATRP, signal amplification, AgNPs, electrochemical biosensor*

INTRODUCTION

Ultrasensitive DNA detection has considerable potential applications in early diagnostic, biological research, and food safety. Many methods for detecting DNA, such as polyacrylamide gel electrophoresis,[1] droplet digital polymerase chain reaction,[2] DNA microarray[3] (gene chip), and so forth, have their own limitations, such as being time-consuming and cumbersome and requiring up to 48 h of meticulous laboratory operations. In order to solve these shortcomings and drawbacks, nucleic acid biosensors have made considerable progress in the past few decades, especially electrochemical DNA biosensors.[4] Among many DNA biosensors, such as photoelectrochemical DNA biosensors,[5] colorimetric DNA biosensors,[6] and fluorescent DNA biosensors,[7] DNA electrochemical biosensors have been favored by many researchers because of their rapid response, low casting, high sensitivity, and good stability.[8,9] However, the existing electrochemical DNA biosensors still have some drawbacks, such as poor stability, high cost, and complex preparation process.

For the purpose of improving the sensitivity of electrochemical DNA biosensors, enzymes,[10] electrochemically active substances,[11] and nanomaterials[12] have been used as markers, and deoxyribonucleic acid[13] (DNA), hairpin DNA,[14,15] morpholine oligonucleotide,[16] locked nucleic acid,[17] molecular beacon,[18] and nanoparticles[19] are used as capture probes. At the same time, in order to improve the sensitivity of electrochemical DNA biosensors, researchers often introduce nucleic acid amplification methods into DNA biosensors, such as strand displacement amplification,[20,21] rolling circle amplification,[22,23] and loop-mediated isothermal amplification.[24] However, existing DNA electrochemical biosensors have been hindered in clinical and practical applications because of their complicated fabrication process, time-consuming reactions, and high cost. Therefore, it is necessary to establish a reliable, rapid, highly sensitive, and simple

Received: May 14, 2019
Accepted: July 17, 2019
Published: July 17, 2019

DOI: 10.1021/acsami.9b08037
ACS Appl. Mater. Interfaces 2019, 11, 27568−27573

method to detect trace DNA, which is not only of great significance in the development of drug biological analysis but also conducive to the in-depth study of disease diagnosis and clinical detection.

Herein, we report a novel method to detect DNA, which used peptide nucleic acid (PNA) as a capture probe and utilized electrochemical atom transfer radical polymerization (eATRP) signal amplification and DNA-templated metal silver deposition. In the presence of T-DNA, the stable PNA/DNA double-stranded structure was formed. After Zr^{4+} binds to phosphate on DNA, the initiator [α-bromophenylacetic acid (BPAA)] of ATRP is attached to PNA/DNA heteroduplexes based on the phosphate groups of T-DNA and carboxylate groups of BPAA via zirconium−phosphate−carboxylate chemistries. A large amount of glyco-syloxyethyl methacrylates (GEMA) was captured on the formed PNA/DNA duplex via the ATRP reaction, and the polymerized sugars were assembled on the electrode surface. The polysaccharides were then oxidized to aldehydes with $NaIO_4$, and silver nanoparticles (AgNPs) deposited onto the electrode surface by the silver mirror reaction. Finally, the results indicate that the peak current of AgNPs deposited on T-DNA increases linearly as the logarithm of T-DNA concentration increases in the range of 1 pM to 10 aM with a low detection limit, excellent stability, selectivity, and specificity. Moreover, the sensor is successfully used to detect DNA in actual serum samples with satisfactory results, which indicates huge promise for detecting gene biomarkers and clinical analysis.

Scheme 1. Preparation Schematic of the DNA Biosensor Based on SI-eATRP Signal Amplification and DNA-Templated Silver Particles

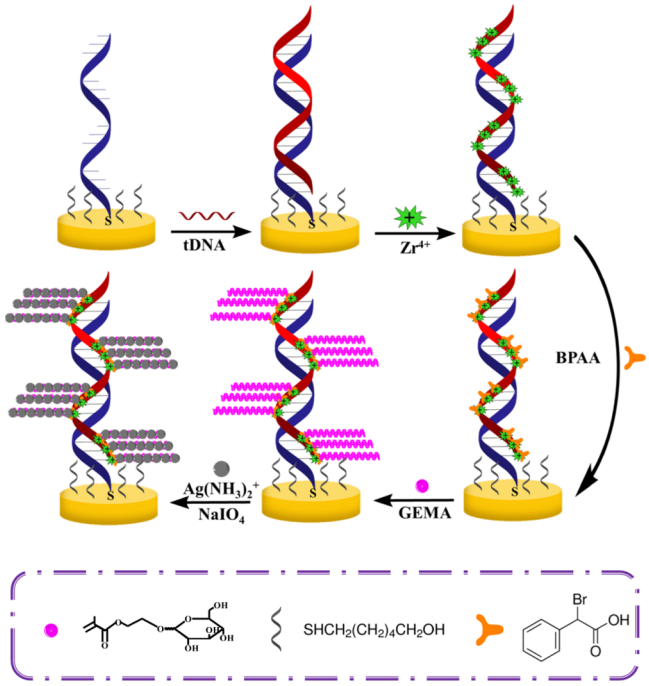

EXPERIMENTAL SECTION

Fabrication of the Proposed DNA Biosensor. First, the gold electrode was pretreated,[25] and the electrode modified with BPAA/Zr^{4+}/DNA/MCH/PNA was prepared[26] according to our previous work. The details of the preparation are shown in the Supporting Information. Then, the Au electrode surface was immersed in an eATRP polymerization solution (10 mM GEMA, 10 mM $Cu^{II}Br$, 10 mM Me_6TREN, 1.0 M KBr, and 0.1 M KPF_6), and then subjected to eATRP polymerization at room temperature for 30 min under a potentiostatic condition. After ATRP polymerization, the Au electrode was washed successively with absolute ethanol and ultrapure water to remove residual chemical agents on the surface. Later, the Au electrode was immersed in 25 mM $NaIO_4$ solution for 2 h and washed with ultrapure water. Finally, the surface was immersed in 16 mM $Ag(NH_3)_2OH$ solution for 1 h. Then, the modified electrode was rinsed thoroughly with ultrapure water to obtain an ultrasensitive and novel DNA biosensor platform.

Electrochemical Measurement. The electrochemical signal of Ag was measured by differential pulse voltammetry (DPV) in 1.0 M KCl and the potential range of −0.15 to 0.25 V versus a saturated calomel electrode (SCE). See details in the Supporting Information.

RESULTS AND DISCUSSION

Sensing Principle. The principle of manufacturing an electrochemical biosensor for detecting DNA combining surface-initiated (SI)-eATRP signal amplification strategies with DNA-templated silver particles is shown in Scheme 1. First, the PNA of the 5′-end-labeled thiol group is attached on the Au electrode surface via a Au−thiol interaction. Here, PNA is selected as the capture probe because PNA is neutral charged, and there is no electrostatic repulsion between the DNA. Therefore, the stability and specificity of the binding are greatly improved. Then, the remaining active sites are blocked with MCH on the Au electrode surface. In the presence of T-DNA, the T-DNA was specifically recognized by the PNA probe through the principle of base complementary pairing. After the Zr^{4+} binds to the DNA,[10] the ATRP initiator (BPAA) is added on the Au electrode surface, which can initiate the subsequent eATRP reaction that is carried out in an electrolytic cell by adding GEMA (monomer), Cu (catalyst), and Me_6TREN (ligand of Cu). After half an hour, it is found that a narrower molecular weight distribution of long-chain polymeric sugars is obtained. The ATRP mechanism mediated via the electrochemical control of Cu^I/Cu^{II} conversion and activator generation is shown in Scheme S1. In the redox reaction of Cu^I and Cu^{II}, the catalyst Cu^I serves as a carrier for the bromine atom. The coordination energy between Me_6TREN and Cu^I can affect the position of redox equilibrium, so that the low-oxidized metal halide catalyst (activator), CuBr, can take Br atom from the initiator R−Br (BPAA) and generate the free radical $R^\bullet$ and the high-oxidized metal halide, $CuBr_2$. $R^\bullet$ initiates monomer polymerization to form growth-chain radical R-GEMAn (active species), which can also take Br atoms from $CuBr_2$ and be terminated, forming a temporarily inactivated macromolecular halide R-GEMAn-Br (dormant species). However, the termination reaction is reversible, and R-GEMAn-Br, like the initiator R−Br, can be activated by CuBr to take up the Br atom, reforming the active species (R-GEMAn$^\bullet$). In this way, a reversible equilibrium is established between the dormant species (macromolecule halides) and the active species (free radicals), so that the concentration of free radicals in the system is greatly reduced, thereby avoiding the side effects of biradical termination and realizing the control of polymerization.[27] Polysaccharides with narrow molecular weight distribution can be obtained by repeating the above ATRP, and are then oxidized to polyaldehydes via $NaIO_4$. Finally, a large amount of metallic silver adheres to the long-chain polymer material by a silver mirror reaction. Thus, the signal amplification biosensor based

DOI: 10.1021/acsami.9b08037
ACS Appl. Mater. Interfaces 2019, 11, 27568−27573

on eATRP polymerization and DNA-templated silver particles is successfully realized.

Characterization of Electrode Modification. In common polymerization reactions, ascorbic acid is often oxidized to produce some byproducts, such as dehydroascorbic acid, which will affect the purity of the final polymer. Therefore, it is particularly environmentally friendly to avoid the use of chemical agents as reducing agents and to replace them with electricity. In order to investigative the feasibility of DNA detection based on the ATRP signal amplification strategy of PNA as a capture probe, we first determined the constant potential of the catalyst, Cu, in the ATRP reaction, which reduced $Cu^{II}Br/Me_6TREN$ to the potential of Cu^{I}/Me_6TREN. As shown in Figure S1, in the electrolyte of eATRP solution without GEMA, the constant point of Cu was determined via cyclic voltammetry (CV) in the range of −0.9 to 0.4 V (sweep segments: 2, sample interval: 0.001 V, scanning rate: 0.1 V s^{-1}). A reduction peak was observed at −0.55 V potential due to the reduction of $Cu^{II}Br/Me_6TREN$ to Cu^{I}/Me_6TREN. Exploring the effect of Cu^{I} potential on polymerization, when E_{app} > −0.55 V, the polymerization becomes more likely to occur, but the rate of polymerization is significantly slowed down, resulting in a long reaction time, which is not conducive to detection. At the potential of E_{app} < −0.55 V, resulting in an increase in the ratio of $[Cu^{I}Br/Me_6TREN]/[Cu^{II}Br/Me_6TREN]$, more $Cu^{I}Br/Me_6TREN$ appears in the polymerization system; but in this case, the polymerization rate is too rapid, resulting in deterioration of the polymerization reaction, making the polymerization reaction poorly controlled. Therefore, SI-eATRP is carried out under −0.55 V versus SCE.

In addition, the stability constant of the Cu^{I} complex has been reported in the previous literature. In the redox reaction between Cu^{I} and Cu^{II}, Me_6TREN acts as a ligand to coordinate with Cu^{I}, on the one hand, increasing the dissolution of the catalyst Cu^{I} in the organic phase. On the other hand, when Me6TREN is coordinated with Cu^{I}, its oxidation−reduction potential is affected, which can be used to adjust the activity of Cu^{I}, making Cu^{I} more stable in solution and facilitating the ATRP reaction. At the same time, methacrylate is used as a monomer in the ATRP polymerization system, based on its moderate polymerization rate and having all of the characteristics of living polymerization. Compared to other living polymerizations, ATRP polymerization can be carried out at room temperature, which is more practical.

In view of the discussion above, we evaluate the feasibility of the direct detection of DNA based on PNA as a capture probe and utilized eATRP signal amplification and DNA-templated metal silver deposition. The results are shown in Figure 1A; the electrochemical signal of DPV directly indicates the presence or absence of AgNPs. In the absence of T-DNA, a weak current response (b) is observed, which is not significantly different from the bare electrode (a). This indicates that when DNA does not participate in the reaction, subsequent reactions will not happen. When the T-DNA is added, a very strong peak current (d) is observed, the potential of the detected peak is the potential at which AgNPs are oxidized to Ag^{+}. It is then explored that the current is caused by the ATRP amplification strategy, and no current response is detected when the ATRP step is missing (c). This further demonstrates that the ATRP signal amplification strategy can be applied to DNA detection. At the same time, it is verified that the detection method proposed by Scheme 1 is correct and feasible.

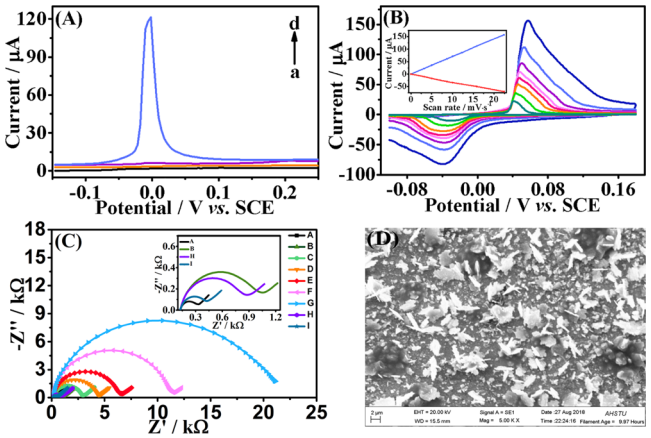

Figure 1. (A) DPV of the PNA/MCH/T-DNA/Zr^{4+}/BPAA/GEMA/$NaIO_4$/Ag-modified Au electrode (d, blue), in the absence of GEMA (c, purple), in the absence of T-DNA (b, orange), and bare Au electrode (a, black). (B) CVs of PNA/MCH/T-DNA/Zr^{4+}/BPAA/GEMA/$NaIO_4$/Ag−Au electrode modified Au electrode in 1.0 M KCl at different scan rates of 10, 25, 50, 75, 100, 150, 250, and 500 mV s^{-1}. Inset: relationship between oxidation (blue line) and reduction (red line) peak currents and scan rates; (C) Nyquist plots of the bare Au electrode (A), PNA (B), PNA/MCH (C), PNA/MCH/T-DNA (D), PNA/MCH/T-DNA/Zr^{4+} (E), PNA/MCH/T-DNA/Zr^{4+}/BPAA (F), PNA/MCH/T-DNA/Zr^{4+}/BPAA/GEMA (G), PNA/MCH/T-DNA/Zr^{4+}/BPAA/GEMA/$NaIO_4$ (H), and PNA/MCH/T-DNA/Zr^{4+}/BPAA/GEMA/$NaIO_4$/Ag modified Au electrode (I). (D) SEM image of the polymer-grafted Au electrode (PNA/MCH/T-DNA/Zr^{4+}/BPAA/GEMA/$NaIO_4$/Ag-modified Au electrode).

In addition, further characterization of the modified Au electrode was performed by CV with scan rate from 10 to 500 mV s^{-1}. It can be seen that as the square root of the scan rate increases, the peak current of the oxidation peak (blue line) increases linearly, whereas the peak current of the reduction peak (red line) decreases linearly (Figure 1B), indicating that the metallic silver is diffusion-controlled on the electrode surface. It is proved once again that the feasibility proposed in Scheme 1 is rational.

Next, electrochemical impedance spectroscopy (EIS) is used to characterize the electrodes modified at different stages. The typical electrochemical interface can be equivalent to the circuit. As shown in Figure 1C, the EIS of the bare Au electrode showed an extremely small semicircular region (curve A), indicating that the charge-transfer process is fast. When the PNA probe modified the Au electrode, the semicircular region increased significantly, and the charge-transfer resistance (R_{ct}) value was about 1.05 kΩ (curve B). The reason for this change may be that the PNA is modified on the surface of the Au electrode to cause an increase of steric hindrance. In curve C, the surface of the Au electrode is blocked with MCH, and the increase of steric hindrance leads to a further increase of resistance. It is worth noting that after the T-DNA is applied to the surface of the Au electrode, the phosphate of the DNA is negatively charged, thereby preventing the diffusion of the $[Fe(CN)_6]^{3-}/[Fe(CN)_6]^{4-}$ probe to the surface of the Au electrode, resulting in an increase in R_{ct} (curve D). As shown in the curve (e), when Zr^{4+} is associated to the electrode surface, the impedance continues to increase, which may be due to the electrostatic interaction between the positively charged Zr^{4+} and the negatively charged $[Fe(CN)_6]^{3-}/[Fe(CN)_6]^{4-}$, leading to the adsorption of $[Fe(CN)_6]^{3-}/[Fe(CN)_6]^{4-}$ onto the PNA/DNA double

DOI: 10.1021/acsami.9b08037
ACS Appl. Mater. Interfaces 2019, 11, 27568−27573

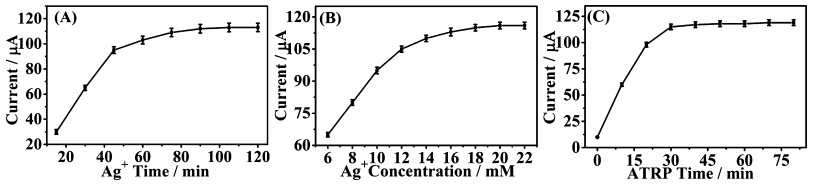

Figure 2. Optimization of the experimental conditions. (A) Effect of in situ metallization of Ag on the DPV response of the biosensor. (B) Effect of Ag^+ concentration on the DPV response of the biosensor. The Ag^+ concentrations were 6, 8, 10, 12, 14, 16, 18, 20, and 22 mM. (C) Effects of different ATRP reaction times.

strands. Then, the adsorbed $[Fe(CN)_6]^{3-}/[Fe(CN)_6]^{4-}$ has electrostatic repulsion effect on charge transfer, resulting in a further increase of impedance. When the initiator BPAA is added, as the hydrophilicity of the surface of the Au electrode is greatly lowered, the impedance value is continuously increased (curve F). Subsequently, a large semicircular region (curve G) is observed when ATRP occurred at the electrode, indicating that large number of sugars accumulated on the Au electrode surface after the ATRP reaction, and polysaccharides may form a film on the Au electrode surface, hindering the electron transfer of the electrochemical probe.[28,29] It is noteworthy that the impedance decreases sharply after adding $NaIO_4$, and the preliminary analysis may be as follows: (1) the film formed on the electrode surface disappears owing to the oxidation of the polymerized sugar to the polymerized aldehyde, and the surface hydrophobicity is greatly increased. (2) The electron-withdrawing effect of the formyl group promotes the transfer of $[Fe(CN)_6]^{3-}/[Fe(CN)_6]^{4-}$ on the Au electrode surface. Because AgNPs have excellent electron conductivity, a sharp decrease in the impedance value (curve I) is observed when Ag was deposited on the electrode, which is similar to that of the bare electrode. This result further proves that each step of the sensor preparation process is successfully carried out.

Finally, the morphology of the Au electrode surface of AgNPs deposited by the DNA template is characterized by SEM. As shown in Figure 1D, the growth of AgNPs is observed only along the DNA strand, and no background Ag deposition occurred because only after the phosphoric acid on the DNA skeleton interacted with Zr^{4+}, the DNA−Ag complex could be formed through the above series of reactions. Furthermore, as shown in Figure S2, electronic differential system further confirmed that the nanoparticles in the DNA helix are AgNPs. The results show that the formation of AgNPs on the DNA backbone could be regarded as an electroactive substance in subsequent electrochemical experiments, which is consistent with the results of electrochemical detection.

Optimization of Experimental Condition. Several factors in this sensing system are considered to affect the sensitivity of DNA biosensors. Therefore, in order to improve the sensitivity of the sensor, we optimized the experimental parameters in the system to obtain the optimal experimental conditions.

As the DPV response of AgNPs is closely related to the concentration of T-DNA, the generation of AgNPs is worthy of discussion. The formation and growth of AgNPs on the surface of the electrode is caused by the polymerization of the aldehyde group to reduce silver ions, which then further extended by Ostwald ripening. This phenomenon was first proposed by Wilhelm Ostwald. It describes the evolution of a heterophase structure over time; the smaller crystalline or sol particles in the solute dissolve and redeposit onto the larger crystalline or sol particles.

Take the AgNPs in this experiment as an example; all atoms in AgNPs are tightly linked to the 12 atoms adjacent thereto, forming a very stable structure, whereas the atoms on the surface of the AgNPs are greatly reduced in stability because there are less than 12 adjacent atoms. Depending on the fact that large particles have lower energy, therefore larger crystals will have more stable structures than smaller ones. Because the thermodynamic system continuously performs the process of releasing energy, the atoms on the surface of the smaller crystal tend to break away from the crystal according to the Kelvin equation and dissolve in the solvent. If all small crystals go through this process, the concentration of free atoms in the solvent will be greatly increased, and when the free atoms in the solvent reach supersaturation, they will have a tendency to condense to the surface of large crystals.[30] Therefore, the small particles will continue to shrink in the solvent, whereas the relatively large particles will continue to increase, and the overall average radius of the solute will also increase. It can be assumed that after a sufficiently long time, all solutes will eventually become a giant spherical particle to achieve the smallest surface area.

Although high silver concentrations can provide a large number of silver cores, their physical stability mainly depends on the time given to their Ostwald ripening, which takes quite a long time to establish AgNPs and is not practicable for real biosensor applications. If the silver concentration is too low, the resulting bridge structure is unstable or the formed structure is scattered, and it is easy to collapse under hydrodynamic action. Ultimately, the size of the resulting AgNPs can be controlled by the length of the process. Therefore, it is necessary to optimize the duration and concentration of silver deposition.

In view of the discussion above, the time and concentration of silver deposition will determine the sensitivity of the biosensor and therefore be optimized. As shown in Figure 2A, the current signal increases sharply from 15 to 45 min, which is due to surface adsorption kinetics, and the sharply increasing current signal may be owing to the continued growth of silver particles by Ostwald's mature kinetics. It tends to be flat after 90 min, which may be owing to the possibility of an overlapping crossover between 45 and 90 min. Considering that we are developing a fast-responding electrochemical biosensor, the optimal time for in situ metallization in subsequent experiments is 60 min. In addition, the concentration of silver ammonia solution is also an important factor affecting the sensitivity of the sensor. Therefore, the influence of silver concentration on the current signal is further studied. As shown in Figure 2B, the signal of the current increases sharply with increasing silver concentration from 6 to 12 mM. In the silver concentration range from 12 to 18 mM,

DOI: 10.1021/acsami.9b08037
ACS Appl. Mater. Interfaces 2019, 11, 27568−27573

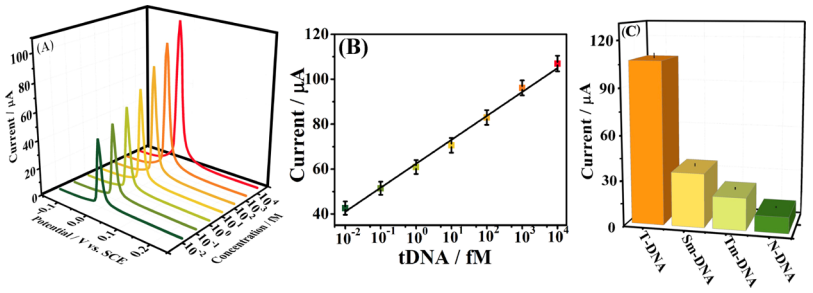

Figure 3. (A) DPV of different concentrations of T-DNA in the range from 10 aM to 10 pM. (B) Corresponding calibration curve of (A). (C) DPV responses at the potential of 0 V toward T-DNA, Sm-DNA, Tm-DNA, and N-DNA (10 pM).

the signal of the current slowly increases until a plateau appears. Therefore, 16 mM is used as the optimum concentration of the silver ammonia solution. Furthermore, there is no doubt that the current signal reflects the number of nanoparticles, which is related to the amount of polymerized aldehydes. Therefore, the amount of sugar polymerized via the ATRP will directly affect the performance of the modified biosensor. To this end, we optimized the reaction time of ATRP. As observed from Figure 2C, with the increase of reaction time, the electrochemical signal is higher, and it tends to be stable when the time reaches 30 min. Therefore, we chose 30 min as the best time for the ATRP reaction.

Quantitative Analysis of Target DNA. As described above, after the T-DNA is introduced into the electrode, a large amount of metallic silver is introduced into the reaction system through a series of reactions due to the assembly of the DNA with the probe, and the electrochemistry signal is remarkably enhanced. Under optimal detection conditions, DPV experiments were performed in KCl solution (1 M) to evaluate the standard dynamic linear range of DNA prepared by the biosensor. An obvious oxidation current could be seen at the potential of 0 V from Figure 3A, and oxidation current increased with the increase of DNA concentrations. From the calibration plots in Figure 3B, the electrochemical signal of Ag deposited on tDNA linearly increases with increasing logarithm of T-DNA concentration over a range of T-DNA concentrations from 10 pM to 10 aM. The linear fit equation is I (μA) = 62.53 + 10.58 log[$C_{tDNA(fM)}$] (R^2 = 0.992) and the detection limit is estimated to be 4.725 aM (S/N = 3). By comparing the detection results of the biosensor prepared in this experiment with the ones previously reported, as shown in Table S2, the biosensor prepared in this experiment has ultrasensitivity because of SI-eATRP signal amplification strategies.

Moreover, the DPV responses of different DNA sequences (Sm-DNA, Tm-DNA, and Nm-DNA) were compared with that from the T-DNA to evaluate the selectivity of this signal amplification strategy. Figure 3C shows that the electrochemical signals produced by T-DNA with complete complementary sequence are 3.0-fold and 5.0-fold of Sm-DNA and Tm-DNA, respectively; the electrochemical signal generated by N-DNA with completely disordered sequence is very weak and almost identical to the bare electrode, indicating that the DNA electrochemical biosensor has the ability to efficiently recognize single base mismatches. In addition, the DNA electrochemical biosensor has good accuracy and repeatability (the relative standard deviation of six relatively independent electrodes is 2.6%). At the same time, the DNA electrochemical biosensor was stored under a sealed condition of 4 °C for two weeks, and the DPV response still retained 94% of the initial response, showing satisfactory stability.

Sample Analysis. In order to evaluate the analytical reliability and application potential of this strategy in actual serum samples, the interference of complex serum samples on their analytical performance was investigated. We prepared different concentrations of DNA (10 aM, 10 pM, and 10 fM) samples with 10% diluted healthy human serum.

As demonstrated in Table 1, the results showed that the recovery ratio from the samples were excellent, varying from 97.5 to 95.2% with relative standard deviation of 3.7−5.5%, indicating that the method has the potential to determine DNA in clinical analysis.

Table 1. Recovery of DNA in 10% Diluted Normal Human Serum

sample	added	found[a]	recovery ratio (%)
DNA	10 pM	9.75 pM	97.5
DNA	10 fM	9.64 fM	96.4
DNA	10 aM	9.52 aM	95.2

[a]The average of six measured values.

CONCLUSIONS

We developed an ultrasensitive electrochemical DNA biosensor, which utilizes DNA-templated silver deposition and SI-eATRP on Au electrodes. The biosensor can detect the minimum 4.725 aM T-DNA under the optimal conditions and ATRP amplification. The biosensor was also successfully applied to detect DNA in human serum samples. In addition, more optimization is needed to reduce the total measurement time of actual samples in biosensor applications. The significance of this article is to introduce a new electrochemical biosensor and bioassay method. Moreover, the signal amplification can be used for high-sensitivity detection of biomolecules such as proteins and microRNA and will have practical applications in clinical practice.

ASSOCIATED CONTENT

Supporting Information

The Supporting Information is available free of charge on the ACS Publications website at DOI: 10.1021/acsami.9b08037.

Materials and reagents; detailed sequences of oligonucleotides; experimental section; principle of the SI-eATRP-polymerization-based amplification strategy; determination of the constant potential of the catalyst (Cu); traces of the Ag element of the elemental mapping of the modified gold electrode; and comparison of the

DOI: 10.1021/acsami.9b08037
ACS Appl. Mater. Interfaces 2019, 11, 27568−27573

detection limits and linear ranges of DNA biosensors (PDF)

AUTHOR INFORMATION

Corresponding Authors

*E-mail: j.kong@njust.edu.cn. Phone: +86-25-84303109 (J.K.).

*E-mail: zhangxueji@szu.edu.cn. Phone: +86-0755-26537298 (X.Z.).

ORCID

Jinming Kong: 0000-0001-5721-6513

Author Contributions

All authors have given approval to the final version of the manuscript.

Notes

The authors declare no competing financial interest.

ACKNOWLEDGMENTS

This work was financially supported by the National Natural Science Foundation of China (21575066).

REFERENCES

(1) Orita, M.; Iwahana, H.; Kanazawa, H.; Hayashi, K.; Sekiya, T. Detection of Polymorphisms of Human DNA by Gel Electrophoresis as Single-Strand Conformation Polymorphisms. *Proc. Natl. Acad. Sci. U.S.A.* **1989**, *86*, 2766−2770.

(2) Doi, H.; Takahara, T.; Minamoto, T.; Matsuhashi, S.; Uchii, K.; Yamanaka, H. Droplet Digital Polymerase Chain Reaction (PCR) Outperforms Real-Time PCR in the Detection of Environmental DNA from an Invasive Fish Species. *Environ. Sci. Technol.* **2015**, *49*, 5601−5608.

(3) Trio, P. Z.; Kawahara, A.; Tanigawa, S.; Sakao, K.; Hou, D.-X. DNA Microarray Profiling Highlights Nrf2-Mediated Chemoprevention Targeted by Wasabi-Derived Isothiocyanates in HepG2 Cells. *Nutr. Cancer* **2017**, *69*, 105−116.

(4) Drummond, T. G.; Hill, M. G.; Barton, J. K. Electrochemical DNA Sensors. *Nat. Biotechnol.* **2003**, *21*, 1192.

(5) Zhao, W.-W.; Xu, J.-J.; Chen, H.-Y. Photoelectrochemical DNA Biosensors. *Chem. Rev.* **2014**, *114*, 7421−7441.

(6) Yang, X.; Wen, Y.; Wang, L.; Zhou, C.; Li, Q.; Xu, L.; Li, L.; Shi, J.; Lal, R.; Ren, S.; Li, J.; Jia, N.; Liu, G. Hybridization Detection Using a 3D DNA Nanostructured Reporter Probe. *ACS Appl. Mater. Interfaces* **2017**, *9*, 38281−38287.

(7) Loo, A. H.; Sofer, Z.; Bouša, D.; Ulbrich, P.; Bonanni, A.; Pumera, M. Carboxylic Carbon Quantum Dots as a Fluorescent Sensing Platform for DNA Detection. *ACS Appl. Mater. Interfaces* **2016**, *8*, 1951−1957.

(8) Ji, H.; Yan, F.; Lei, J.; Ju, H. Ultrasensitive electrochemical detection of nucleic acids by template enhanced hybridization followed with rolling circle amplification. *Anal. Chem.* **2012**, *84*, 7166−7171.

(9) Zhu, Z.; Lei, J.; Liu, L.; Ju, H. Label-free electrochemical DNA sensing with a one-target-multitriggered hybridization chain reaction strategy. *Analyst* **2013**, *138*, 5995−6000.

(10) Liu, G.; Wan, Y.; Gau, V.; Zhang, J.; Wang, L.; Song, S.; Fan, C. An Enzyme-Based E-DNA Sensor for Sequence-Specific Detection of Femtomolar DNA Targets. *J. Am. Chem. Soc.* **2008**, *130*, 6820−6825.

(11) Liu, G.; Wang, J.; Wunschel, D. S.; Lin, Y. Electrochemical Proteolytic Beacon for Detection of Matrix Etalloproteinase Activities. *J. Am. Chem. Soc.* **2006**, *128*, 12382−12383.

(12) Kong, J.; Ferhan, A. R.; Chen, X.; Zhang, L.; Balasubramanian, N. Polysaccharide Templated Silver Nanowire for Ultrasensitive Electrical Detection of Nucleic Acids. *Anal. Chem.* **2008**, *80*, 7213−7217.

(13) Lu, C. h. H.; Yang, H. h. H.; Zhu, C. h. L.; Chen, X.; Chen, G. h. N. A Graphene Platform for Sensing Biomolecules. *Angew. Chem.* **2009**, *121*, 4879−4881.

(14) Farjami, E.; Clima, L.; Gothelf, K.; Ferapontova, E. E. "Off−On" Electrochemical Hairpin-DNA-Based Genosensor for Cancer Diagnostics. *Anal. Chem.* **2011**, *83*, 1594−1602.

(15) Fan, C.; Plaxco, K. W.; Heeger, A. J. Electrochemical Interrogation of Conformational Changes as a Reagentless Method for the Sequence-Specific Detection of DNA. *Proc. Natl. Acad. Sci. U.S.A.* **2003**, *100*, 9134−9137.

(16) Hudziak, R. M.; Barofsky, E.; Barofsky, D. F.; Weller, D. L.; Huang, S.-B.; Weller, D. D. Resistance of Morpholino Phosphorodiamidate Oligomers to Enzymatic Degradation. *Antisense Nucleic Acid Drug Dev.* **1996**, *6*, 267−272.

(17) Rana, M.; Balcioglu, M.; Robertson, N.; Yigit, M. V. Nanographene Oxide as a Novel Platform for Monitoring the Effect of LNA Modification on Nucleic Acid Interactions. *Analyst* **2014**, *139*, 714−720.

(18) Li, F.; Huang, Y.; Yang, Q.; Zhong, Z.; Li, D.; Wang, L.; Song, S.; Fan, C. A Graphene-Enhanced Molecular Beacon for Homogeneous DNA Detection. *Nanoscale* **2010**, *2*, 1021−1026.

(19) Liu, G.; Lin, Y. Electrochemical Quantification of Single-Nucleotide Polymorphisms Using Nanoparticle Probes. *J. Am. Chem. Soc.* **2007**, *129*, 10394−10401.

(20) Chen, A.; Gui, G.-F.; Zhuo, Y.; Chai, Y.-Q.; Xiang, Y.; Yuan, R. Signal-Off Electrochemiluminescence Biosensor Based on Phi29 DNA Polymerase Mediated Strand Displacement Amplification for MicroRNA Detection. *Anal. Chem.* **2015**, *87*, 6328−6334.

(21) Zhang, J.; Li, C.; Zhi, X.; Ramón, G. A.; Liu, Y.; Zhang, C.; Pan, F.; Cui, D. Hairpin DNA-Templated Silver Nanoclusters as Novel Beacons in strand Displacement Amplification for MicroRNA Detection. *Anal. Chem.* **2015**, *88*, 1294−1302.

(22) Li, X.-Y.; Du, Y. C.; Zhang, Y. P.; Kong, D. M. Dual Functional Phi29 DNA Polymerase-Triggered Exponential Rolling Circle Amplification for Sequence-Specific Detection of Target DNA Embedded in Long-Stranded Genomic DNA. *Sci. Rep.* **2017**, *7*, 6263.

(23) Deng, K.; Li, C.; Huang, H.; Li, X. Rolling Circle Amplification Based on Signal-Enhanced Electrochemical DNA Sensor for Ultrasensitive Transcription Factor Detection. *Sens. Actuators, B* **2017**, *238*, 1302−1308.

(24) Li, J.; Macdonald, J. Advances in Isothermal Amplification: Novel Strategies Inspired by Biological Processes. *Biosens. Bioelectron.* **2015**, *64*, 196−211.

(25) Sun, H.; Qiu, Y.; Liu, Q.; Wang, Q.; Huang, Y.; Wen, D.; Zhang, X.; Liu, Q.; Liu, G.; Kong, J. Ultrasensitive DNA biosensor based on electrochemical atom transfer radical polymerization. *Biosens. Bioelectron.* **2019**, *131*, 193−199.

(26) Sun, H.; Xu, W.; Liu, B.; Liu, Q.; Wang, Q.; Li, L.; Kong, J.; Zhang, X. DNA Ultrasensitive Detection via SI-eRAFT and In Situ Metallization Dual-Signal Amplification. *Anal. Chem.* **2019**, *91*, 9198.

(27) Matyjaszewski, K. Atom Transfer Radical Polymerization (ATRP): Current Status and Future Perspectives. *Macromolecules* **2012**, *45*, 4015−4039.

(28) Yang, Q.; Xu, Z.-K.; Hu, M.-X.; Li, J.-J.; Wu, J. Novel sequence for generating glycopolymer tethered on a membrane surface. *Langmuir* **2005**, *21*, 10717−10723.

(29) Yang, Q.; Tian, J.; Dai, Z.-W.; Hu, M.-X.; Xu, Z.-K. Novel photoinduced grafting-chemical reaction sequence for the construction of a glycosylation surface. *Langmuir* **2006**, *22*, 10097−10102.

(30) Ratke, L.; Voorhees, P. W. *Growth and Coarsening: Ostwald Ripening in Material Processing*; Springer, 2002.

DOI: 10.1021/acsami.9b08037
ACS Appl. Mater. Interfaces 2019, 11, 27568−27573